**International Journal of Environment, Agriculture and Biotechnology**
Vol-8, Issue-4; Jul-Aug, 2023
Peer-Reviewed International Journal
Journal Home Page Available: https://ijeab.com/
Journal DOI: 10.22161/ijeab

# A Change Analysis of Land Use and Carbon Storage in Maoming Based on the InVEST Model and GIS

Wanying Liang, Ruei-Yuan Wang*

School of Sciences, Guangdong University of Petrochem Technology(GDUPT), Maoming 525000, China

*Corresponding author

Received: 25 Jun 2023; Received in revised form: 21 Jul 2023; Accepted: 30 Jul 2023; Available online: 07 Aug 2023



***Abstract*— With the increasing attention paid to ecological and environmental issues, the monitoring and exploration of carbon storage have become increasingly important in ecosystems, attracting numerous attentions from academia and industry. Based on the era background of "double carbon", this study first discussed and sorted out the relevant theories, analyzed the changes and characteristics of various categories in the study area based on land use data, and analyzed the spatial-temporal changes of carbon storages in Maoming City from 1980 to 2020 through transfer matrix and dynamic degree analysis and the InVEST model to explore the impact of land use change on carbon storages. The analysis results show that there is a positive correlation between carbon storage and vegetation coverage, and the transfer of arable land and forest land is the main reason for the decrease in carbon storage. Therefore, it is recommended to pay attention to optimizing land use structures and controlling the expansion of construction land caused by urbanization in order to achieve the goal of protecting the ecological environment.*

***Keywords*— Integrate Valuation of Ecosystem Services and Tradeoffs（InVEST）：Land Use/Cover Change (LUCC); Carbon Storage; Transfer Matrix; Dynamic Degree.**

## I. INTRODUCTION

The improvement of the economic level and scientific and technological progress promote the development of human society while also bringing negative impacts to global climate change and triggering human thinking on sustainable development. Since the industrial revolution, the global climate has worsened day by day. The main reason is that the excessive use of fossil fuels, deforestation, land reclamation, overgrazing, and other irrational land use patterns have led to an increasing number of greenhouse gases in the atmosphere. Therefore, human economic activities exceed the carbon sequestration rate of the system itself, becoming the primary factor affecting the carbon storage of ecosystems (Huang, 2015). The inducing factors that affect carbon storage can be divided into two categories. One is economic factors such as the expansion of infrastructure construction scale, the growth of residents' consumption, and the transformation of land use methods. Another type is policy incentives, which lead to phenomena such as short-lived construction, large-scale demolition and construction, and low-density construction (Huang et al., 2021)。

Land is the foundation of human survival and development, as well as the most important natural resource. With the development of the social economy and the gradual advancement of urbanization, land use has become a topic of great concern. Many studies have shown that land use change is an important reason for the change in ecosystem carbon storage, which leads to a large amount of carbon flowing from the terrestrial ecosystem to the atmospheric ecosystem (Gao and Wang, 2019). In addition, in the process of urbanization, the expansion of urban construction land is caused by land use changes caused by the occupation of forest land, arable land, and grassland, which also makes the urban ecosystem face serious carbon loss problems.

The impact of urban land use change on the ecosystem has been a hot topic in the field of ecology in recent years. Among them, carbon storage is an important link in the ecosystem service function. Vegetation and soil are the two most important carbon pools of the terrestrial ecosystem, and their carbon fixation function plays an important role in alleviating the climate crisis (Bi et al., 2010). Land carbon storage, as an important link in ecosystems, is also a target of concern for many scholars (Poska et al., 2008). For example, Huang (2015) and Zhu et al. (2021) elaborated on the characteristics of land use change, dynamic changes in carbon storage, and the relationship between land use and carbon sequestration, providing references for conducting carbon storage research.

Liu et al. and Ren et al. (2021), based on remote sensing data, obtained the carbon density of Gansu Province by correcting the national carbon density. The modified carbon density was inputted into the InVEST model to estimate the carbon storage of Gansu Province from 1990 to 2015. The impact of land use change on carbon storage was analyzed, indicating that land use change has a significant impact on carbon storage. Luo et al. (2023) coupled the PLUS and InVEST model to study the multi-environmental land use changes and their impact on carbon storage in Xi'an, indicating that the significant expansion of construction land and the encroachment of ecological land and arable land are the main reasons for the loss of carbon storage in the ecosystem. Li and Luo (2023) used the InVEST model to reveal the impact of construction land expansion on regional ecosystem carbon storage in the Karst Plateau region of central Guizhou, China, indicating the impact of urban expansion on carbon storage.

In summary, the InVEST model has become a very popular analytical method for studying carbon storage in ecosystems. In addition, it shows that there are relatively more studies on carbon storage changes targeting countries or provinces, while there is less discussion on carbon storage changes at the city or county level. Based on this, this study will take Maoming City as the research area, explore the relationship between land use change and carbon storage in different periods of time, and provide scientific data references for the optimization of land use structure in Maoming City, as well as response methods to the national "double carbon" goal. Therefore, this study aims to analyze and discuss the land use change and carbon storage of Maoming City from 1980 to 2020 through remote sensing data and the InVEST model, so as to understand the change in carbon emissions caused by land use change.

## II. STYDY AREA

Maoming is located in the southwest of Guangdong Province, bordering Yangjiang City in the east, Yunfu City in the northeast, Guangxi in the north and west, and Zhanjiang City in the south. It is one of the most important coastal cities in Guangdong. The terrain is high in the north and low in the south, sloping from northeast to southwest, and located in the south of the Tropic of Cancer. The mountains, hills, platforms, and plains are clearly layered, accounting for 11.2%, 55.8%, 6.6%, and 13.85% of the total land area of the city, respectively. The rivers in this area are developed (Figure 1), accounting for 12.6% of the city's area.

Maoming's petrochemical industry, led by oil refining and ethylene production, occupies an important position in the country. At the beginning of 1959, Maoming's shale mining area gradually developed into an "oil city" with the petrochemical industry as its industry, becoming an important petrochemical production and export base in southern China and an important energy, raw materials, and heavy chemical industry base in Guangdong Province. Rich mineral resources are one of its major characteristics. There are 57 types of minerals identified in the jurisdiction of Maoming, among which the development and processing of mineral resources such as "Nanyu" and kaolin have distinct advantages and characteristics. The total area of the city is 11458 square kilometers, accounting for about 6.4% of the province's total area. As of 2022, the population had reached 6.238 million people. The development of mineral resources has accelerated the urbanization process, and after decades of urban expansion, land use changes have also had significant changes and impacts.

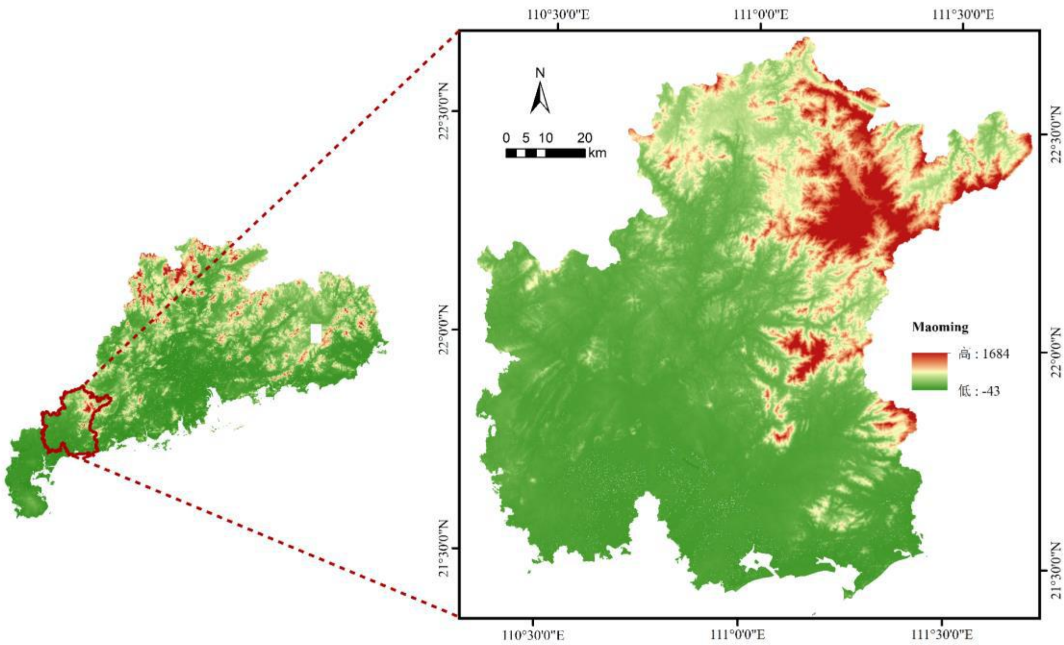


*Fig.1 Location and Topographic Map of Maoming City*

## III. MATERIALS AND METHODS

### 3.1 Data Sources

The analysis data used in this research are mainly LUCC data from 1980 to 2020, which are from the Institute of Geographic Sciences and Resources, Chinese Academy of Sciences (Table 1).

*Table 1 Data Sources and Use Applications*

| Data type | Data source | Applications |
|---|---|---|
| 1980-2020 Maoming LUCC data | Institute of Geographic Sciences and Resources, Chinese Academy of Sciences (http://www.resdc.cn) | Produce land use data for five periods |

### 3.2 Methods

This study is based on the land use data of Maoming in 1980, 1990, 2000, 2010, and 2020. The main steps are as follows (Figure 2):

1) Using land use data import ArcGIS and clip to obtain LUCC data for the study area from 1980 to 2020.

2) Reclassify 23 classification data into 6 categories, including arable land, forest land, grassland, water bodies, construction land, and unused land. Finally, process the grid row and column numbers and projection coordinate system in ArcGIS to ensure consistency with other driving factor data.

3) The reclassified grid files are vectorized, fused, and intersected to obtain the land use transfer matrix from 1980 to 2020 and calculate the area change and dynamic degree between different years.

4) Through a literature review, based on previous experience and according to the carbon density correction formula, carbon density data in the Maoming region was obtained.

5) Process the parameters required for the carbon storage and storage module of the InVEST model, and obtain carbon storage and land use grid data. And based on this, obtain a carbon storage map and use ArcGIS to create a spatial distribution map of carbon storage from 1980 to 2020.

6) Finally, according to the analysis data of the land use transfer matrix and the InVEST model, a comprehensive analysis is carried out.

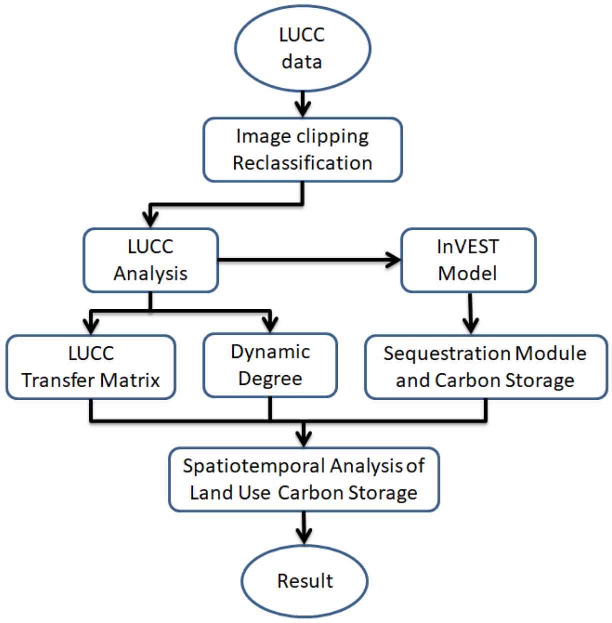


*Fig.2 The Schema of the Study*

### 3.3 Land Use Transfer Matrix

The land use transfer matrix (Table 2) is derived from the quantitative description of system state transfer in system analysis (Yu, 2018). Usually, the land use type at time $T_1$ is represented in rows, and the land use type at time $T_2$ is shown in a list. $P_{ij}$ represents the percentage of the area converted from land type i to land type j in the total land area between $T_1$ and $T_2$. $P_{ii}$ represents the percentage of land types that remain unchanged from $T_1$ to $T_2$. $P_{jj}$ represents the percentage of land types that remain unchanged from $T_1$ to $T_2$. Pi+ represents the total area percentage of land type i at time $T_1$. $P_{+j}$ represent the total area percentage of j types of land use at the $T_2$ time point.

$P_{i+}$–$P_{ii}$ is the percentage decrease in land type i area between $T_1$ and $T_2$. $P_+j$–$P_{jj}$ is the percentage increase in j area during $T_1$ to $T_2$ (Liu and Zhu, 2010).

*Table 2 Land Use Transfer Matrix Model*

| $T_1$ | | $T_2$ | | | | $P_{i+}$ | Decrease |
|---|---|---|---|---|---|---|---|
| | | $A_1$ | $A_2$ | A | $A_n$ | | |
| | $A_1$ | $P_{11}$ | $P_{12}$ | … | $P_{1n}$ | $P_{1+}$ | $P_{1+}$—$P_{11}$ |
| | $A_2$ | $P_{21}$ | $P_{22}$ | … | $P_{2n}$ | $P_{2+}$ | $P_{2+}$—$P_{22}$ |
| | ⋮ | ⋮ | ⋮ | ⋮ | ⋮ | | |
| | $A_n$ | $P_{n1}$ | $P_{n2}$ | … | $P_{nn}$ | $P_{n+}$ | $P_{n+}$—$P_{nn}$ |
| $P_{+j}$ | | $P_{+1}$ | $P_{+2}$ | … | $P_+$ | 1 | |
| **Newly added** | | $P_{+1}$—$P_{11}$ | $P_{+2}$—$P_{22}$ | … | $P_{+n}$—$P_{nn}$ | | |

**3.4 Dynamic Degree Model**

The regional differences in the rate of land use change can be expressed using a land use dynamic degree model, which represents the changes in land types within a certain time range in the study area, reflecting the magnitude and speed of regional land change. Through the dynamic degree changes in different periods, the characteristics of land use change can be studied, as shown in formula (1).

$$S=\left\{\sum_{ij}^{n}\left(\frac{\Delta S_{i-j}}{S_i}\right)\right\}\times\left(\frac{1}{t}\right)\times 100\% \quad (1)$$

Where formula (1), $S_i$ is the total area of type i land use type at the monitoring start time, $\triangle S_{i-j}$ is the total area of type i land use type conversion converted to other land use types during the period from the monitoring start to the monitoring end, t is the meaning of time period (a) n, and S is the land use change rate of the study sample area corresponding to time period t. This model can also be used to measure the change rate of a single land use type (Liu et al., 2003). When analyzing the net change and land use conversion of land use types, the area per unit grid is taken as $S_i$, and the net change conversion area of each type is taken as ΔSi-j, forming the basis for the classification of change maps and conversion type maps.

**3.5 InVEST Model**

The comprehensive evaluation model of ecosystem services and transactions, referred to as the InVEST model (Integrate Valuation of Ecosystem Services and Tradeoffs, InVEST 3.1), was jointly developed by the World Wide Fund for Nature (WWF), Stanford University, and the Nature Conservancy (TNC) in 2007, aiming to balance the balance between human activities, economic benefits, and the development of natural laws through different land use/cover scenarios and to simulate and evaluate the value of regional ecosystem services to provide support for government decision-making. This paper selects the carbon storage and fixation module of the terrestrial ecosystem to study the change in carbon emissions caused by land use change in Maoming.

**3.5.1 Carbon Storage and Fixation Module**

The necessary data for this model is land use/cover data, which must be in grid .img or .tif format (unit: meters). The unit of density table for the four major carbon sinks is tons /per hectare, and the table is in CSV format.

The total carbon storage in ecosystems is composed of four basic carbon pools: above-ground biomass, underground biomass, soil carbon pool, and dead organic matter. The above-ground biomass includes tree trunks, branches, etc.; the underground biomass includes the root system of vegetation; the soil carbon pool includes various types of organic carbon in the soil; and dead organic matter includes dead or fallen trees and fallen materials (Hou et al., 2020). By obtaining the carbon density of the four basic carbon pools of different land use/cover types, multiplied by the grid area of each land type, and then converting it to obtain the carbon storage amount per unit area, the expression of carbon storage per unit area is generally expressed in kg/㎡ or t/hm$^2$. The operating formulas for the four basic carbon sinks are as follows:

$$C_{\text{total}} = C_{\text{above}} + C_{\text{below}} + C_{\text{soil}} + C_{\text{dead}} \quad (2)$$

In the formula (2):$C_{\text{total}}$: Total carbon storage; $C_{\text{above}}$: carbon storage capacity of above ground parts; $C_{\text{below}}$: represents the underground carbon storage capacity; $C_{\text{soil}}$: represents the amount of organic carbon stored in the soil; $C_{\text{dead}}$: represents the storage amount of dead organic matter carbon.

### 3.5.2 Carbon Storage Data

The InVEST model requires the input of land use data and carbon density values in the study area to form a carbon pool. Data on the general dead organic carbon pool is difficult to obtain (Chuai et al., 2011), so this study refers to the three basic carbon pools. The selection of carbon density data and the accuracy of future land use change simulation plans largely determine the accuracy of the final carbon storage results. Therefore, the determination of carbon density mainly refers to previous studies, and the carbon density data of the study area is obtained by consulting the literature. Because the study area is relatively smaller than the whole country and the literature is lacking, previous studies believe that the difference in carbon density of land types in the same climate zone is small, and the required data can be calculated in areas with similar land use types and climate characteristics (Zhou et al., 2018).

Thus, this study uses the carbon density results of land types in the Guangdong area calculated by Wu et al. (2016) and Lin et al. (2022). The carbon density data of the local land type is corrected by the formula, and the carbon storage density of Maoming is obtained by inversion. Moreover, studies at home and abroad have shown that both biomass carbon density and soil organic carbon density have a significant positive correlation with annual precipitation, while the correlation with annual average temperature is weak. The selection of the formula is mainly based on the universality of the formula and the closeness of the temperature and precipitation in the study area to Guangdong Province. The correction factor calculation formula (Mwambala et al., 2023) is (3), (4), and (5) ：

$$K_{BP} = \frac{C'_{BP}}{C''_{BP}} \qquad K_{BT} = \frac{C'_{BT}}{C''_{BT}} \quad (3)$$

$$K_B = K_{BP}K_{BT} = \frac{C'_{BP}}{C''_{BP}} \times \frac{C'_{BT}}{C''_{BT}} \quad (4)$$

$$K_S = \frac{C'_{SP}}{C''_{SP}} \quad (5)$$

In the formulas (3), (4),and (5), $K_{BP}$、$K_{BT}$ represent the vegetation carbon density precipitation factor and air temperature correction coefficient; $K_B$ represents the above-ground and underground vegetation carbon density correction coefficient; $K_S$ represents the soil carbon density correction coefficient; and $C'$、$C''$ represent the carbon densities of Maoming and Guangdong, respectively, which are calculated by substituting the annual average temperature and annual precipitation into formulas (6), (7), and (8).

$$C_{BP} = 6.798e^{0.0054MAP} \quad (6)$$

$$C_{BT} = 24MAT + 398 \quad (7)$$

$$C_{SP} = 3.3968MAP + 3996.1 \quad (8)$$

(6), (7), and (8), where: MAP represents precipitation; MAT represents temperature; $C_{BP}$ 、 $C_{BT}$ represent vegetation carbon density obtained from precipitation and temperature, respectively; and $C_{SP}$ represents soil carbon density obtained from precipitation. The comprehensively obtained carbon density values for each land type are shown in Table 3.

*Table 3 Carbon Density of Different Land Use Types in Maoming (Unit: t/hm2)*

| Land use type | Aboveground carbon density | Underground carbon density | Soil carbon density | Dead organic matter carbon density |
|---|---|---|---|---|
| Arable land | 40.37 | 8.28 | 11.43 | 0.00 |
| Forest land | 49.34 | 15.1 | 20.32 | 2.82 |
| Grass land | 41.18 | 219.73 | 10.53 | 0.24 |
| Water bodies | 0.72 | 0.97 | 3.19 | 1.24 |
| Construction land | 28.94 | 5.95 | 18.94 | 0.00 |
| unutilized | 35.70 | 7.32 | 5.62 | 0.00 |

## IV. ANALYSIS AND RESULTS

### 4.1 Land Use Change

Through ArcGIS analysis, the land use map of Maoming in five phases from 1980 to 2020 is obtained (Figure 3). According to the classification results, the main types of land use are arable land, forest land, grassland, water bodies, construction land, and unused land. Arable land is concentrated in the southern region; forest land is most widely distributed, concentrated in the north, and also distributed in coastal areas on both sides; construction land is concentrated in each urban area, with Dianbai District and Maonan District being the most prominent. Overall, from 1980 to 2020, the most significant type of land use change was forest land, distributed in the central and southern regions.

International Journal of Environment, Agriculture and Biotechnology
Vol-8, Issue-4; Jul-Aug, 2023
Peer-Reviewed International Journal
Journal Home Page Available: https://ijeab.com/
Journal DOI: 10.22161/ijeab

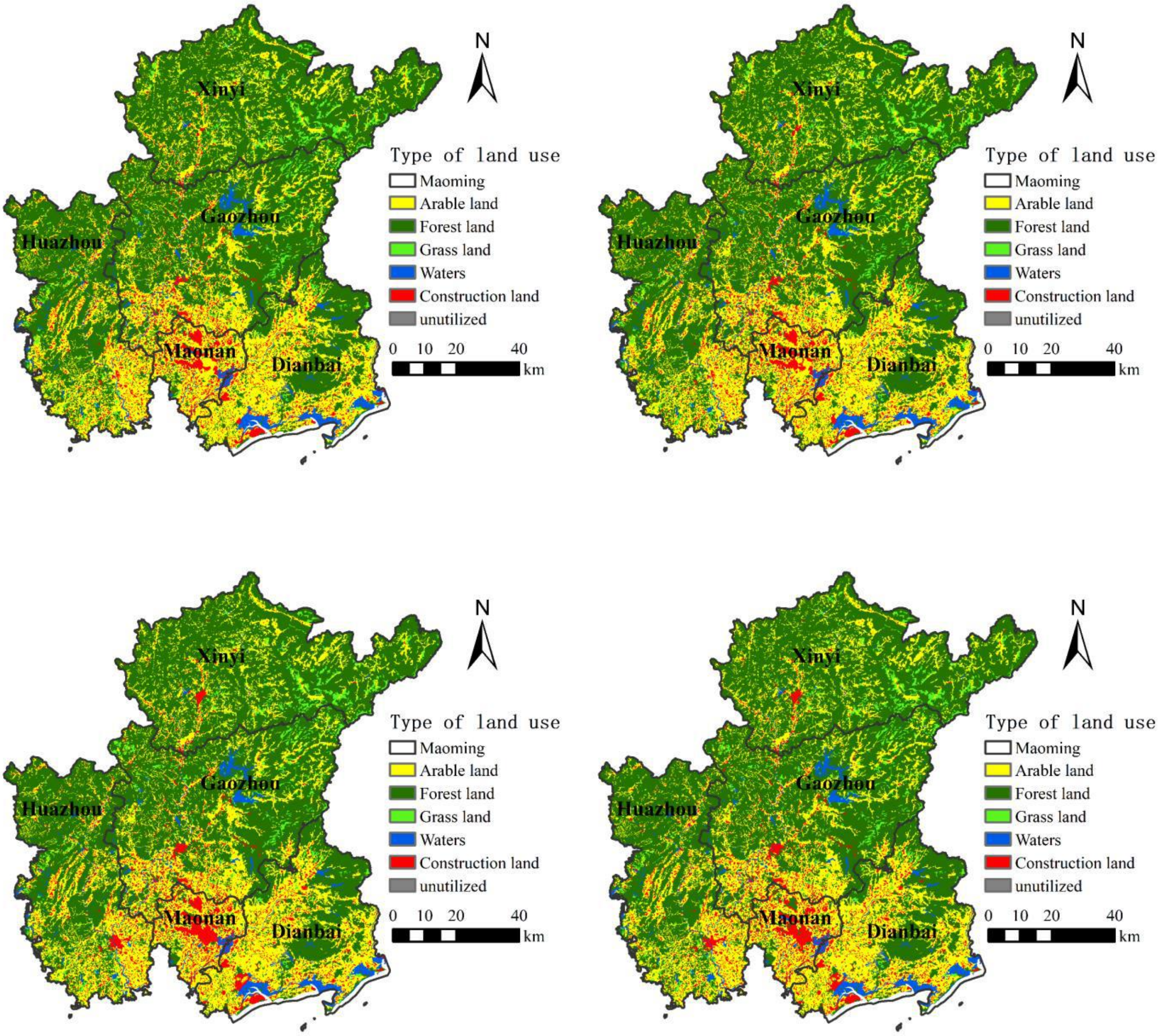

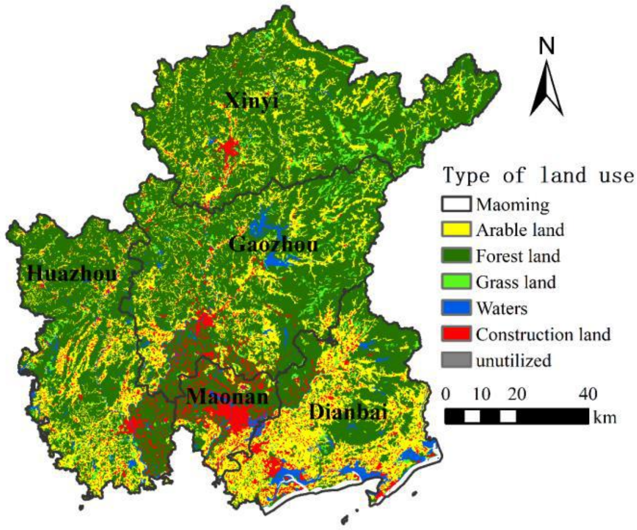


*Fig.3 Land Use Map of Maoming from 1980 to 2020*

**4.1.1 Forest Land is Advantageous Type**

Through analysis, the land type area and land use change matrix from 1980 to 2020 are obtained (Table 4 and Table 5). The data shows that forest land is the largest land use type in Maoming, with an area of 7230.9km². The proportion is 58.8–63.6%, which is a dominant land use type. In 1980, the transferred areas of arable land, forest land, grassland, water bodies, construction land, and unused land were 858.5 km², 230.3km²，50.4 km²，43.9 km²，89.3 km² and 6.7 km²；In 2020, the transferred areas of arable land, forest land, grassland, water bodies, construction land, and unused land were 164.0 km², 777.3 km²，43.9 km²，73.6 km²、218.9 km² and 1.5 km².

*Table 4 Area (km²）and Rate (%) of Land Types in Maoming from 1980 to 2020*

| Type | 1980 | | 1990 | | 2000 | | 2010 | | 2020 | |
|---|---|---|---|---|---|---|---|---|---|---|
| | Area | Rate | Area | Rate | Area | Rate | Area | Rate | Area | Rate |
| Arable land | 3372.4 | 29.7% | 3360.8 | 29.6% | 3306.9 | 29.1% | 3295.7 | 29.0% | 2677.8 | 23.6% |
| Forest land | 6683.2 | 58.8% | 6682.9 | 58.8% | 6678.5 | 58.8% | 6703.9 | 59.0% | 7230.9 | 63.6% |
| Grass land | 352.5 | 3.1% | 353.5 | 3.1% | 349.8 | 3.1% | 339.5 | 3.0% | 346.0 | 3.0% |
| Water bodies | 320.8 | 2.8% | 322.3 | 2.8% | 324.4 | 2.9% | 332.6 | 2.9% | 351.0 | 3.1% |
| Construction land | 621.7 | 5.5% | 630.9 | 5.6% | 689.8 | 6.1% | 679.2 | 6.0% | 753.2 | 6.6% |
| unutilized | 12.1 | 0.1% | 12.1 | 0.1% | 13.0 | 0.1% | 12.8 | 0.1% | 6.9 | 0.1% |

*Table 5 Transfer Matrix of Land Use in Maoming from 1980 to 2020 (Unit: km²)*

| 1980/2020 | Arable land | Forest land | Grass land | Water bodies | Construction land | Unused | Total |
|---|---|---|---|---|---|---|---|
| Arable land | -- | 682.6 | 4.5 | 31.2 | 140.0 | 0.2 | 858.5 |
| Forest land | 108.6 | -- | 33.5 | 27.3 | 59.9 | 1.1 | 230.3 |
| Grass land | 4.8 | 40.7 | -- | 2.8 | 2.1 | -- | 50.4 |
| Water bodies | 9.5 | 19.3 | 1.9 | -- | 13.1 | 0.1 | 43.9 |
| Construction land | 40.8 | 34.4 | 2.0 | 12.2 | -- | 0.0 | 89.3 |
| Unutilized | 0.3 | 0.3 | 2.0 | 0.2 | 3.8 | -- | 6.7 |
| Total | 164.0 | 777.3 | 43.9 | 73.6 | 218.9 | 1.5 | -- |

### 4.1.2 Change Condition of Forest Land

The order of changes in land use types from 1980 to 2020 is arable land>forest land>construction land>water bodies>grassland>unused land, with the highest reduction in arable land, with a total reduction of 694.5km². Secondly, the grassland has decreased by 6.5km², reducing unused land by 5.2km². The largest increase in area was in forest land, with an increase of 547.7 km² from 58.8% in 1980 to 63.6% in 2020, followed by construction land, with an increase of 131.5 km². Then there was the water body, with an increase of 30.2 km². The data shows that the expansion degree of forest land has obvious characteristics compared to other land types.

Through analysis, the land change map of Maoming (Figure 4) is obtained. The data shows that the transformation between arable land, forest land, and construction land is the main feature of land use change in Maoming. The total area transferred out accounts for 39.3% of the total area of transferred land. Among them, the transfer of arable land is the main body of land transfer, which is distributed in the south, including Dianbai District and Huazhou City, and also in the north and middle. The distribution of forest land conversion areas is scattered and evenly distributed in the form of small patches. The area of grassland transferred out is distributed in the northeast of Maoming, and the transfer pattern is relatively concentrated. Overall, the land use conversion rate changed significantly from 2010 to 2020, with arable land, grasslands, and water bodies showing a degradation trend, while construction land, unused land, and forest land showed an expansion trend.

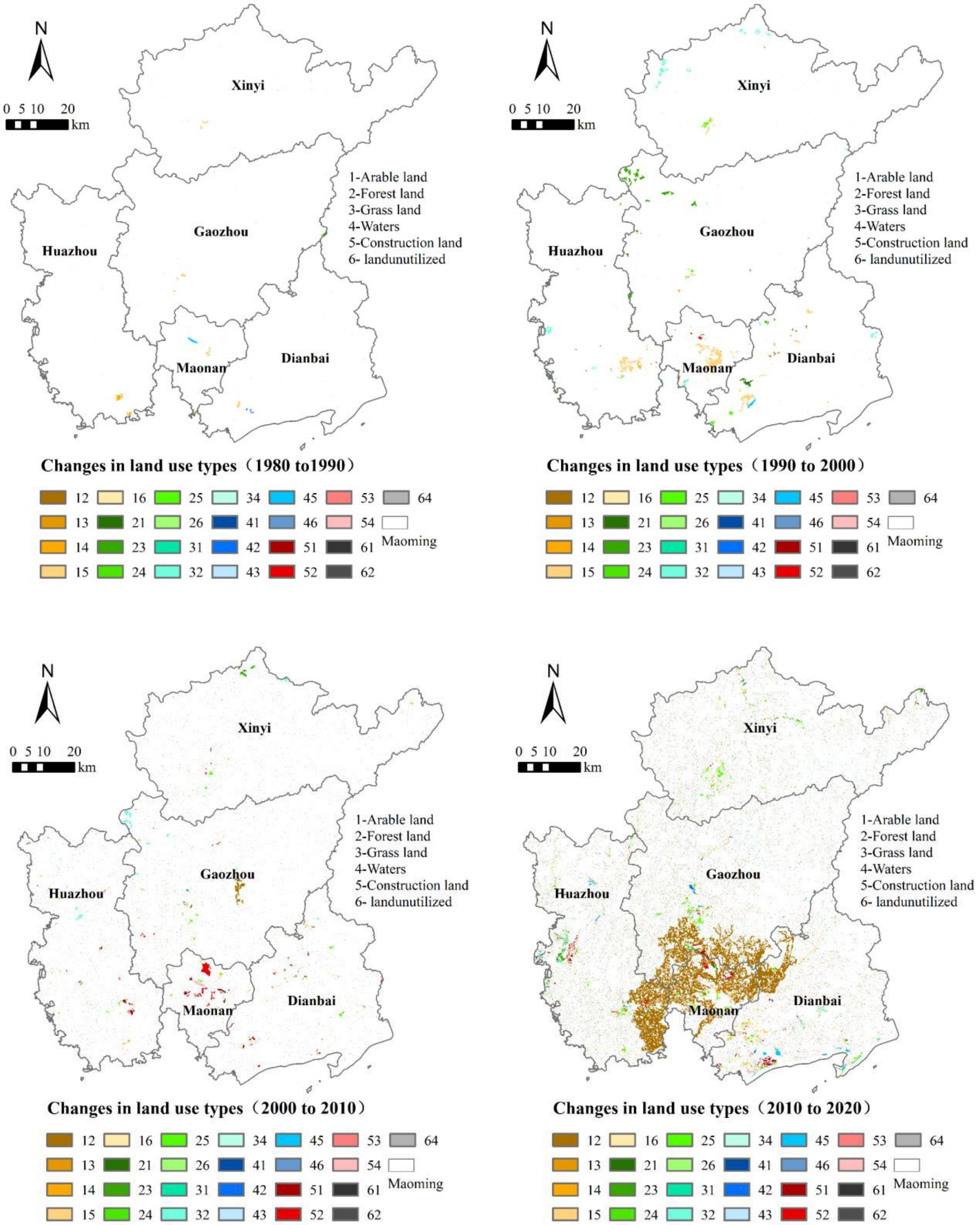


*Fig.4 Land Change Map of Maoming*

Through analysis, we can get the change in land type area and dynamic degree in Maoming from 1980 to 2020, as shown in Table 6. The land dynamics from 2010 to 2020 were relatively high, at 38.73%; the dynamic degree of land use was the lowest from 1980 to 1990, at 1.99%; the total area of unused land remains basically unchanged, while the total area of construction land and forest land shows an increasing trend. From 1980 to 2020, the highest dynamic land type was unused land, accounting for 55.38%, followed by construction land, arable land, water bodies, forest land, and grassland, with proportions of 23.28%, 21.03%, 9.19%, 8.31%, and 6.18%, respectively.

Among the types of land use, forest land, water bodies, and construction land show an increasing trend, while grassland, arable land, and unused land show a decreasing trend. From 1980 to 2020, the main feature of land use type change in Maoming was the increase of forest land, followed by construction land. From 1980 to 1990, in the early stages of reform and opening up, this stage was a period of continuous economic development. In response to an adaptation to the reform and opening up, humans extensively cultivated wasteland, resulting in a reduction in wasteland area. After 2000, due to rapid socio-economic development, continuous population growth, and the promulgation of government policies, the demand for land by humans continued to increase, leading to the expansion of construction land and a sharp decrease in arable land. With the adverse effects of economic development, such as severe environmental pollution and ecological damage, the government has taken a series of policy measures to promote ecological construction and environmental protection. As a result, from 2000 to 2020, the area of forest and grassland increased, and the speed of urban expansion slowed down. This has also increased the protection of the water environment and promoted the restoration of the ecological environment.

*Table 6 Change Area (Km²) and Dynamic Degree (%) of Land Type from 1980 to 2020*

| Type/Year | 1980-1990 | | 1990-2000 | | 2000-2010- | | 2010-2020 | |
|---|---|---|---|---|---|---|---|---|
| | Change | Dynamic Degree | Change | Dynamic Degree | Change | Dynamic Degree | Change | Dynamic Degree |
| Arable land | -11.6 | -0.34% | -53.9 | -1.60% | -11.2 | -0.34% | -617.9 | -18.75% |
| Forest land | -0.3 | -0.01% | -4.4 | -0.07% | 25.4 | 0.38% | 527.0 | 7.86% |
| Grass land | 1.0 | 0.28% | -3.7 | -1.03% | -10.3 | -2.95% | 6.5 | 1.92% |
| Water bodies | 1.4 | 0.45% | 2.2 | 0.67% | 8.2 | 2.53% | 18.4 | 5.54% |
| Construction land | 9.2 | 1.49% | 58.9 | 9.34% | -10.7 | -1.55% | 74.1 | 10.90% |
| unutilized | 0.0 | 0.12% | 0.9 | 7.30% | -0.2 | -1.75% | -5.9 | -46.21% |

### 4.2 Changes in Carbon Storage

The carbon density data of land type in Maoming was obtained by consulting relevant literature and formula correction, and the carbon storage data of 1980–2020 was obtained by importing the carbon storage and storage module of the InVEST model in combination with the data of land use type (Figure 5). The total carbon storage for five years is 92027540.92t, 92032739.8t, 91893990.21t, 91715459.31t, and 93182099.04t, respectively. Overall, carbon storage decreased by 312081.61t from 1980 to 2020, with a decreasing trend from 1990 to 2010 and an increasing trend from 2010 to 2020. This should be related to the increase in forest land mentioned above.

In general, the regional carbon storage changed dramatically from 1990 to 2000. During this period, Maoming's economy grew rapidly, urbanization accelerated, and the demand for land development was also strong. Forest land and arable land were developed and used, resulting in carbon loss. After 2010, the expansion of construction land tends to ease, and land change gradually stabilizes. In response to national environmental protection policies, the restoration of ecological parks is increasing, which presents a favorable situation for the increase of carbon storage.

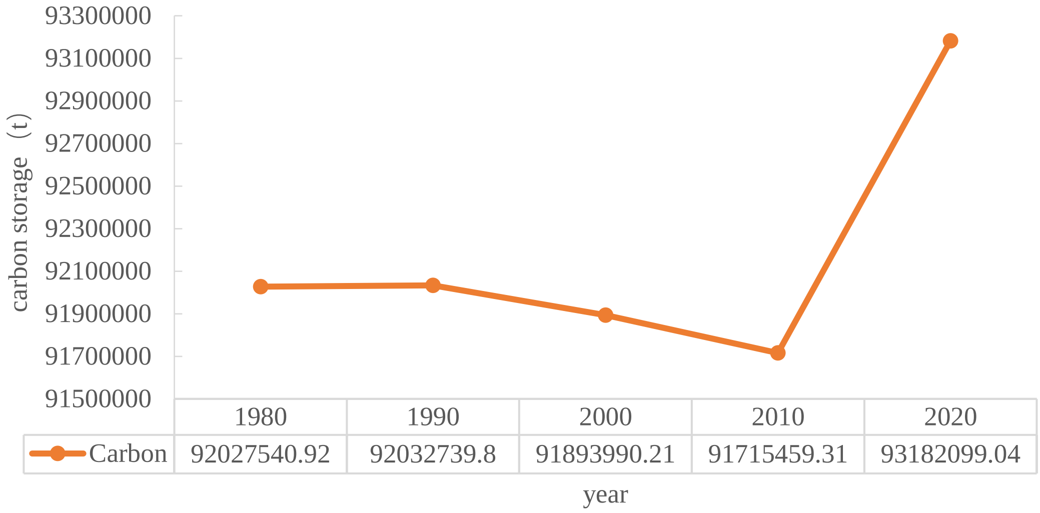


*Fig.5 Change of Terrestrial Carbon Storage in Maoming from 1980 to 2020*

**4.3 Spatial Variation Characteristics of Carbon Storage**

After calculation, the distribution of terrestrial carbon storages in Maoming is obtained (Figure 6). The results show that the regions with high carbon storages are distributed in the north, west, and east, namely the north of Huazhou City, Gaozhou City, and Xinyi City. The carbon storages in the south are relatively low and are distributed in Maonan District, Dianbai District, and the south of Huazhou City. This is because the northern region has high vegetation coverage and relatively high altitude, which is not conducive to urban expansion, is conducive to the generation of carbon storages, and is not easy to lose. The northern region has a relatively high altitude, with landscapes such as Tianma Mountain, Shigen Mountain, and Xianren Cave, as well as a high coverage of forest land area. There are also mountain ranges developed in the eastern and western regions. Low carbon storage areas are mainly concentrated in the arable land, water bodies, construction land, and other areas in Maonan District, which are mostly plain areas with flat terrain suitable for human social production activities, relatively low vegetation coverage, and weak carbon sequestration capacity.

From the perspective of spatial changes in carbon storage, the changing regions exhibit a scattered distribution characteristic. From 1980 to 2000, the regions with significantly reduced carbon storage were distributed in the central and western regions of Huazhou, the northwest of Xinyi, the southeast of Dianbai, and the southwest of Maonan District. During this period, the expansion of construction land was intense, and a large amount of arable land and forest land were converted into construction land. After 2010, the urban expansion capacity gradually decreased, the land type remained relatively stable, and the changes in carbon storage also tended to stabilize. There was a significant increase in regional distribution in the central and western regions of Huazhou, the northwest of Gaozhou, and the western regions of Dianbai. According to the data analysis, the distribution pattern of carbon storage in Maoming during the five phases was obtained (Figure 7), in which the arable land showed a downward trend, with the largest decline from 2010 to 2020; the overall growth trend of forest land is showing, with a relatively fast growth rate from 2010 to 2020; and the carbon storage of construction land areas has steadily increased, which should be related to urban greening. In general, the carbon storage of Maoming declined significantly before 2010, but the decline gradually slowed after 2010, and the overall carbon storage change was relatively moderate.

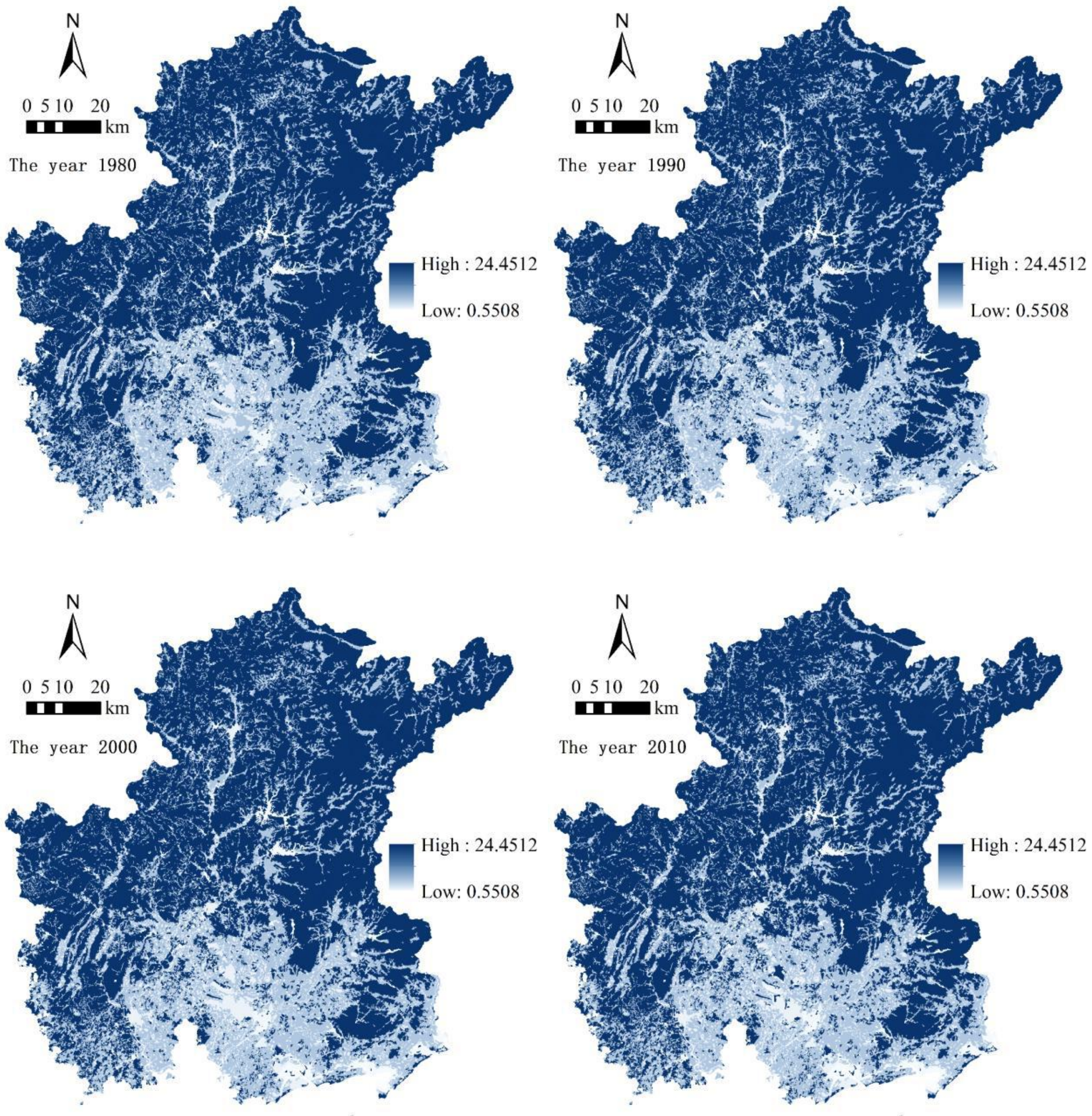

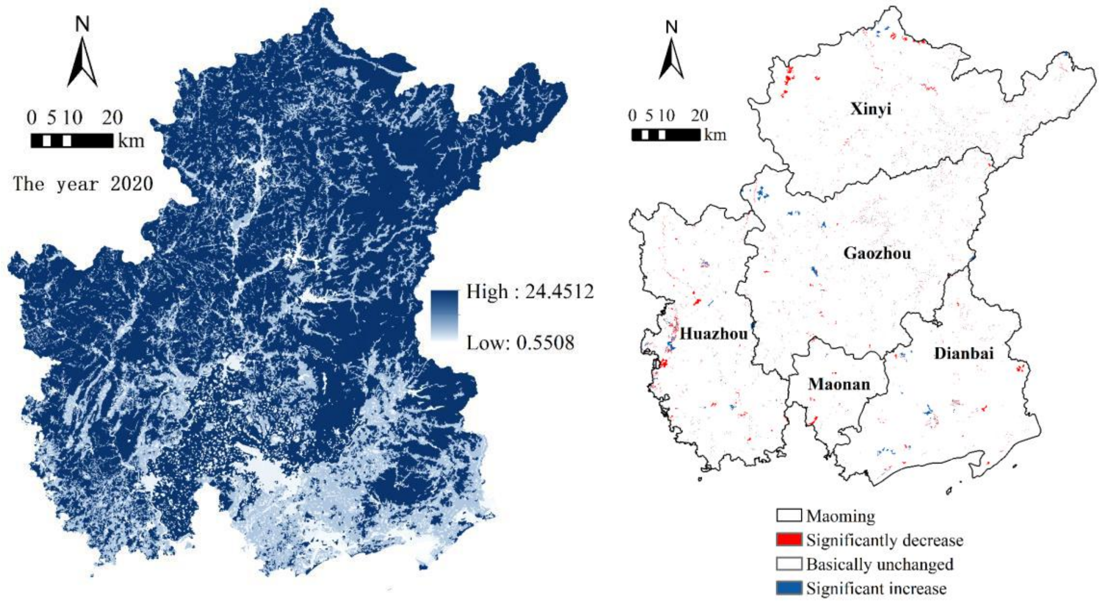


*Fig.6 Spatial Change of Terrestrial Carbon Storage in Maoming*

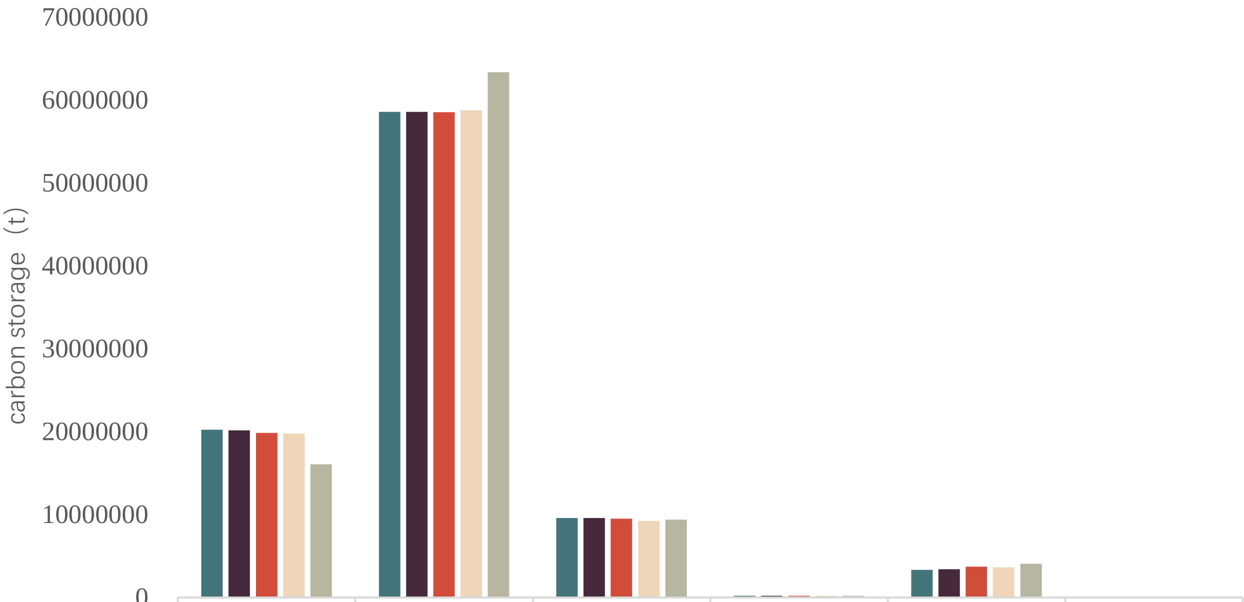


| | Arable land | Forest land | Grass land | Waters | Construction land | unutilized |
|---|---|---|---|---|---|---|
| 1980 | 20257871.296 | 58591870.677 | 9576214.865 | 196335.402 | 3346461.894 | 58786.787 |
| 1990 | 20188465.216 | 58588911.814 | 9603037.832 | 197217.233 | 3396250.874 | 58856.828 |
| 2000 | 19864460.247 | 58550691.200 | 9503790.409 | 198536.398 | 3713360.704 | 63151.254 |
| 2010 | 19797373.469 | 58773323.912 | 9223261.786 | 203563.550 | 3655892.874 | 62043.721 |
| 2020 | 16085818.721 | 63393481.347 | 9400043.966 | 214841.179 | 4054539.002 | 33374.820 |

1980 1990 2000 2010 2020

year

*Fig.7 Change of Carbon Storage in Maoming in Five Periods*

## V. CONCLUSION

This study analyzes the land use types of Maoming over five periods and uses two models of transfer matrix and dynamic degree of land use change to collate and summarize the data. According to the LUCC data from 1980 to 2020, forest land is the dominant land use type in the area, with the largest changes in the area of arable land and forest land, reaching 694.5 $km^2$ and 547.7 $km^2$, followed by construction land. The transformation of these three types of land use change is the most significant. Meanwhile, by analyzing carbon storage data from five periods using the InVEST model, the spatial pattern of carbon storage distribution was obtained, mainly showing the characteristics of high carbon storage in the north and low carbon storage in the south. The conversion between carbon storage and different land use types has a close relationship that is directly proportional to vegetation coverage. The high coverage in the north indicates good carbon sequestration ability.

Overall, the carbon storage in this research area has shown an increasing trend over the past 40 years, from a total of 92027540.92 tons in 1980 to a total of 93182099.04 tons in 2020, with a cumulative value-added of 1154558.12 tons. Among them, arable land and forest land are the most important carbon pools in Maoming. However, with the acceleration of urbanization, a large amount of arable land has been reclaimed, which has become the main reason for carbon loss in this area. With the increase in forest land in 2020, carbon storage capacity has been enhanced, and carbon storages have also increased.

## ACKNOWLEDGEMENTS

The author is grateful for the research grants given to Ruei-Yuan Wang from GDUPT Talents Recruitment (No.2019rc098), and ZY Chen from Talents Recruitment of GDUPT (No. 2021rc002), in Guangdong Province, Peoples R China, and Academic Affairs in GDUPT for Goal Problem-Oriented Teaching Innovation and Practice Project Grant No.701-234660.

## REFERENCES

[1] Huang, H.; Wu, X.; and Cheng, X. The Prediction of Carbon Emission Information in Yangtze River Economic Zone by Deep Learning. *Land*. 2021; 10(12):1380. https://doi.org/10.3390/land10121380

[2] Bi, X., Li, Y., Gao, Q., Wan, Y., and Qin, X. Views and Responding Suggestions on Reducing Emissions from Deforestation and Forest Degradation in Developing Countries. Advances In Climate Change Research, 2010, 6(01):65-69.

[3] Gao, J, and Wang, L. Embedding spatiotemporal changes in carbon storage into urban agglomeration ecosystem management d A case study of the Yangtze River Delta, China. Journal of Cleaner Production, 2019, 237(C).

[4] Poska, A., Sepp, E., Veski, S. and Koppe K. Using quantitative pollen-based land-cover estimations and a spatial CA_Markov model to reconstruct the development of cultural landscape at Rõuge, South Estonia. Veget Hist Archaeobot 17, 527–541 (2008). https://doi.org/10.1007/s00334-007-0124-8

[5] Zhou, R., Lin, M., Wu, Z., and Gong, J. Responses of ecosystem carbon stocks to land use change on the west side of the Pearl, 2018, 37(06):175-183. DOI:10.14108/j.cnki.1008-8873.2018.06.023.

[6] Zhu, Z., Ma, X., and Hu, H. Spatio-temporal evolution and prediction of ecosystem carbon stocks in Guangzhou city by coupling FLUS-INVEST models. Bulletin Soil and Conservation, 2021, 41(2):222-229+239.DOI:10.13961/j.cnki.stbctb.2021.02.0

30.

[7] Chuai, X., Huang, X., Zheng, Z., Zhang, M., Liao, Q., Lai. L., and Lu, J. Land Use Change and Its Influence on Carbon Storage of Terrestrial Ecosystems in Jiangsu Province. Resources Science, 2011, 33(10):1932-1939.

[8] Mwambala, A. N., Nyundo, B. A., and Elikana, E. Tree biomass, carbon stock characteristics and ground beetles (Coleoptera: Carabidae) diversity in the Uzungwa Scarp Forest Nature Reserve, Tanzania. Environmental management, 2023, 71(1):190-200. DOI: 10.1007/s00267-022-01733-5

[9] Lin, T., Yang, M., Wu, D., Liu, F., Yang, J., and Wang, Y. (School of Geography Science and Remote Sensing, Guangzhou University, Guangzhou 510006, China). Spatial correlation and prediction of land use carbon storage based on the InVEST-PLUS model- A case study in Guangdong Province. China Environmental Scince, 2022, 42(10):4827~4839.

[10] Wu, P. J., Liu, X. P., Li, X, and Chen, Y. Impact of urban expansion on carbon storage in terrestrial ecosystems based on InVEST model and CA: A case study of Guangdong Province. China. Geogr. Geo-Inf. Sci, 2016, 32(05): 22-28+36+2..

[11] Li, Y., and Luo, H. Research on carbon storage change of construction land expansion in central Guizhou's karst region based on InVEST model. Journal of Northwest Forestry University, 2023, 1-13.

[12] Ren, X., Pei, T., Chen, Y., Xie, B., and Cheng, D. Impact of land use change on carbon storage in Gansu Province based on carbon density correction. Ecological Science, 2021, 40(4): 66–74. DOI:10.14108/j.cnki.1008-8873.2021.04.008

[13] Liu, Y., Xi, M., Zhang, X., Yu, Z., and Kong, F. Carbon storage distribution characteristics of wetlands in China and its influencing factors. Chinese Journal of Applied Ecology, 2019, 30(07):2481-2489. DOI:10.13287/j.1001-9332.201907.036.

[14] Yu, S. Influencing Factors of Grassland LUCC (Land－Use and Land－Cover Change) based on Land Transfer Matrix—Taking Xilinhaote as an example. Journal of Inner Mongolia Forestry Science & Technology, 2018, 44(01):52-55.

[15] Liu, R., and Zhu, D. Methods for Detecting Land Use Changes Based on the Land Use Transition Matrix [J]. Resources Science, 2010, 32(08):1544-1550.

[16] Liu, J., Liu, M., and Zhuang, D. Study on spatial pattern of land-use change in China during 1995-2000, Science in China (Series D), 2003, 46(4):1373-384.

[17] Huang, H. Analysis on land use change an carbon storage based on InVEST model. China University of Geosciences (Beijing), 2015.

[18] Luo, S. Q., Hu, X. M., Sun, Y., Yan, C., and Zhang, X. Multi-scenario land use change and its impact on carbon storage based on coupled Plus-Invest model[J]. Chinese Journal of Eco-Agriculture, 2023, 31(2): 300−314.

[19] Hou, G, Delang, C. O., Lu, X., and Gao, L. A meta-analysis of changes in soil organic carbon stocks after afforestation with deciduous broadleaved, sempervirent broadleaved, and conifer tree species. Annals of Forest Science 77, 92 (2020). https://doi.org/10.1007/s13595-020-00997-3